IEPC-95-234

# The Role of Spot Mode Transition in the Anode Fall of Pulsed MPD Thrusters

K.D. Diamant*, E.Y. Choueiri† and R.G. Jahn‡
Electric Propulsion and Plasma Dynamics Laboratory
Princeton University
Princeton, New Jersey 08544

## Abstract

An experimentally based description of the major mechanism regulating the anode fall of a high-power, pulsed, self-field MPD thruster is presented. Plasma property data recorded to within one electron Larmor radius of the anode indicate that, with increasing current, the anode transitions from a diffuse, low anode fall mode of operation to a mode with high anode falls and spotty current attachment. The transition is marked by an order of magnitude increase in ion saturation current noise measured in the anode region, which is attributed to spot motion, and, for the case of a smooth anode surface, is triggered by the condition at which the required current density to the anode surface exceeds that which is thermally available. Experiments with a roughened anode indicate that the anode fall in the spot mode serves the purpose of evaporating anode material and that the size of the anode fall in the spot mode should be dependent on anode thermal properties. Comparison of anode falls measured with smooth copper, aluminum, and molybdenum anodes confirms this dependence. The spot mode is also found to provide a mechanism for the saturation of the anode fall and the resultant decrease of the anode power fraction with increasing thruster power.

## 1 Introduction

High power MPD thrusters offer high thrust density ($10^4$ to $10^5$ N/m$^2$) at specific impulses in the range of 1000 to 5000 seconds and have been shown to be advantageous for a number of near Earth and interplanetary missions [1, 2, 3, 4, 5]. In general, these mission studies assume efficiencies of at least 50 percent over mission times between 1000 and 10000 hours, capabilities that have yet to be demonstrated in the laboratory [6]. Major performance limiters with regard to efficiency are frozen flow and anode losses, and even though the fraction of thruster power deposited in the anode can be as low as 10 to 20 percent for operation at a few megawatts [7, 8], anode heat fluxes of several kW/cm$^2$ [9] represent a serious problem for anode lifetime. The primary mechanism for anode power deposition is electron current conduction, and the dominant contributor to the energy of electrons entering the anode surface is the anode fall.

It is well known that, while it is desirable to operate at high values of $J^2/\dot{m}$ (where $J$ is the discharge current and $\dot{m}$ is the mass flow rate) in order to achieve high exhaust velocity and relatively high efficiency, a critical value exists above which a sharp increase in thruster voltage, thruster voltage oscillations, and component erosion occurs. A number of authors have suggested that this phenomenon is due, in part, to anode processes triggered by propellant starvation in the anode region. Hügel [10] has shown experimentally that operation above the critical $J^2/\dot{m}$ results in an abrupt increase in the anode fall and that the critical $J^2/\dot{m}$ varies inversely with the square root of the atomic mass of the propellant. Hügel also presents the results of an MHD model, in which the critical $J^2/\dot{m}$ is identified as that at which the gas pressure at the anode wall decreases to zero, and is found to vary inversely with the square root of the propellant atomic mass. Baksht et al. [11] obtain a similar result, again with an MHD formulation. Hügel suggests that $J^2/\dot{m}$ represents a ratio of magnetic pumping to gasdynamic pressures, and that when magnetic pumping depletes the anode region of propellant to the extent

*Graduate Student, Department of Mechanical and Aerospace Engineering, Member AIAA
†Chief Scientist and Lab Manager, Member AIAA
‡Professor, Department of Mechanical and Aerospace Engineering, Fellow AIAA

that the thermal current density at the anode surface becomes comparable to the discharge current density, the anode transitions from a diffuse to a spot mode of conduction. This idea is echoed by Vainberg et al. [12] who suggest that the sudden increase in the anode fall and the appearance of oscillations correspond to the condition at which the thermal and discharge current densities become comparable, and that the anode fall then heats, vaporizes, and ionizes anode material, resulting in the formation of an anode spot.

A global scaling parameter for thruster operation that may provide additional physical insight into anode behavior is that provided by Choueiri with regard to Alfvén's hypothesis of critical ionization [13]. Choueiri identifies a current, which he labels the critical ionization current $J_{ci}$, corresponding to effective full plasma ionization by equating the electromagnetic thrust $bJ_{ci}^2$ ($b = (\mu_o/4\pi)\ln(r_a/r_c)$, where $r_a$ and $r_c$ are the anode and cathode radii respectively) to the product of the thruster mass flow $\dot{m}$ and propellant species critical ionization velocity $u_{ci}$ (given by $(2\epsilon_i/M)^{1/2}$, where $\epsilon_i$ is the first ionization potential and $M$ is the atomic mass of the propellant species). The identification of a critical $J^2/\dot{m}$ which again exhibits an inverse dependence on the square root of the propellant atomic mass is possible through this formulation, suggesting that the onset of full ionization may impact the anode propellant distribution. Kuriki has shown that a sudden increase in the anode fall, along with the appearance of spectral lines corresponding to anode (and cathode) erosion products correspond to the saturation of argon ion emission (for the case in which most of the propellant is injected near the cathode) [14]. Malliaris et al. obtain remarkable agreement between the critical value of $J^2/\dot{m}$ for the onset of unstable thruster operation and the parameter $u_{ci}/b$ for a variety of propellants and anode to cathode radius ratios [15]. Further, they find that the thruster exhaust velocity corresponding to critical operation is given quite closely by $u_{ci}$, independent of thruster geometry as would be anticipated from the relation for the exhaust velocity $u_{crit}$ at the critical $J^2/\dot{m}$:

$$u_{crit} = \frac{bJ_{ci}^2}{\dot{m}} = u_{ci} \qquad (1)$$

Perhaps neutrals in the anode region, due to their relatively lower collisional coupling with electrons, are not strongly influenced by magnetic pumping, and, following thermal ionization, constitute a source of plasma which postpones starvation (it is unlikely that argon neutrals are ionized within the anode fall, since our measured anode falls at conditions prior to starvation generally lie below the first ionization potential of argon, and the expected spatial extent of the anode fall—order microns—leads to an unrealistically large requirement for the ionization rate). The ratio $J/J_{ci}$, designated $\xi$ by Choueiri [16], will be used to scale most of the data presented here.

Although it is not possible to tell from our work (single thruster geometry, single propellant species), scaling of anode phenomena with $\xi$ is probably an oversimplification. A number of studies [17, 18, 19] have shown that adjustments in thruster operation (propellant injection geometry, electrode length) which should have only minor influence on $J_{fi}$ result in major shifts in the critical current required for the onset of thruster voltage oscillations and increased thruster impedance. For the case in which most of the propellant is injected near the anode, Kuriki [14] shows that, although argon ion emission saturates at approximately the same current as it did for near-cathode injection, the current at which the anode fall abruptly increases and at which electrode erosion products appear is substantially increased.

In this paper we present data which indicate the presence of two modes of anode current attachment. The anode fall is shown to be a Debye-sheath phenomenon, with mode transition occuring at sheath current saturation for a smooth anode. Mode transition is accompanied by abrupt increases in the anode fall and in thruster noise. An explanation for the source of the noise and for the behavior of the anode fall after transition is provided.

## 2 Experimental Facility

A description of the experimental facility and probe diagnostics (triple Langmuir and magnetic probes) is provided in Ref[20]. The most relevant details are repeated here for the convenience of the reader.

The quasisteady pulsed MPD thruster is housed in a cylindrical plexiglass tank of volume 1.12 $m^3$ with an inner diameter of 0.91 m. Prior to thruster firing, the tank is pumped down to approximately 0.04 Pa ($3\times10^{-4}$ torr) by a 15 cm oil diffusion pump and two mechanical pumps. Power is supplied to the thruster by a 160 kJ LC pulse-forming network capable of producing a rectangular current pulse of up to 52 kA for 1 msec. The propellant supplied is argon.

The thruster (Figure 1) consists of a cylindrical plate anode and a 2 percent thoriated tungsten cathode. The anode has an outer diameter of 19 cm, an inner diameter of 10 cm and a thickness of 1 cm.

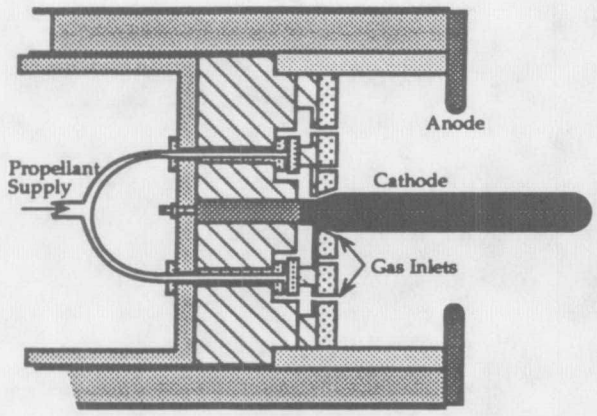


Figure 1: Schematic of MPD thruster.

The inner radius of the anode is machined to a semi-circular lip. The cathode is 10 cm long with a 1.8 cm diameter. The thrust chamber is 5 cm deep with an inner diameter of 12.6 cm. Equal amounts of propellant are injected through twelve equispaced 3 mm diameter holes at a radius of 3.8 cm in the boron nitride backplate and through an annulus surrounding the cathode.

All reported probe measurements have been recorded at the anode lip.

# 3 Results and Discussion

## 3.1 Mode Transition

### 3.1.1 Plasma Properties

Values of the plasma potential with respect to anode potential recorded at 0.1 mm from the anode surface are shown in Figure 2a as a function of $\xi$ (mass flow rates of 4 g/s Ar at currents of 8, 12, 16, and 20 kA, and 6 and 16 g/s Ar at 8, 12, 16, 20, and 24 kA—power levels from 320 kW to 4 MW). These values are expected to represent potential differences across a Debye-scale sheath (Debye length on the order of 1 micron) at the anode surface since estimates of the electron Larmor radius (based on magnetic field measurements taken 1 mm from the anode surface and temperature measurements 0.1 mm from the surface) vary from 0.1 to 0.5 mm for the operating conditions shown and estimates of the electron-ion mean free path are larger than the electron Larmor radius by the factors shown in Figure 2b (electron Hall parameters). At a $\xi$ value of approximately 0.8 a transition

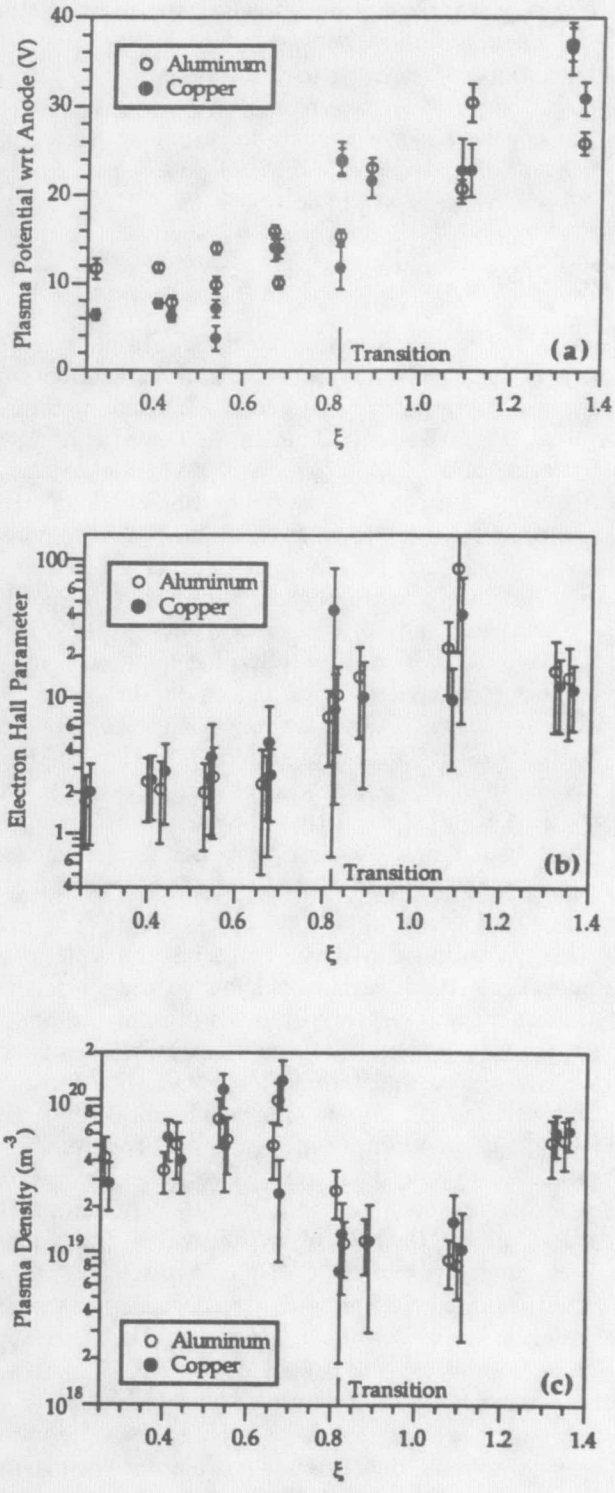


Figure 2: a) Plasma potentials at 0.1 mm, b) Electron Hall parameters at 0.5 mm, and c) Plasma densities at 0.1 mm for aluminum and copper anodes. Some data points in plots b and c have been shifted in $\xi$ value by 0.01 or less to clarify error bar placement.

is observed from operation with sheath potentials below 16 volts to conditions in which the sheath potential assumes values between 20 and 40 volts. This transition corresponds to the sudden appearance of large values of the electron Hall parameter (Figure 2b) and an abrupt decrease in plasma density (Figure 2c). The resurgence of the plasma density for $\xi > 1.3$ will be discussed in section 3.2.4.

### 3.1.2 Noise

The transition is also marked by an abrupt increase in discharge noise. A survey of ion saturation current fluctuations near the anode was conducted for $\xi$ values from 0.44 to 1.33 at a mass flow rate of 6 g/s (currents of 8, 12, 16, 20, and 24 kA). In general the frequency content of these fluctuations is dominated by broad noise in the range of 100 to several hundred kHz. In addition, smaller peaks occur often at frequencies of approximately 2, 3, 4, and 7 MHz (the Nyquist frequency of the experiment was 10 MHz). Similar results have been obtained by several other authors (particularly with regard to the order 100 kHz oscillations), who have found that the strongest fluctuations occur near the anode [21], that the fluctuation intensity scales with power deposited in the anode sheath [22], and that the current at which oscillations are first observed increases as the fraction of propellant injected near the anode increases [23].

Figure 3 shows amplitudes of a number of the previously mentioned MHz peaks (arbitrary units) normalized by the dc level of the ion saturation current as a function of distance from the (aluminum) anode surface (i. e. a number of consistently observed peaks are charted as their amplitude varies with distance from the anode). In the interest of simplicity, a distinction is made only between peaks observed at $\xi$ values above transition and those below transition, regardless of peak center frequency (approximately 2, 3, 4, or 7 MHz both above and below transition). Two things are evident from this figure. The first is that the noise level increases monotonically as the anode surface is approached, indicating that the source of the noise is close to the anode surface. The second is that the noise at conditions above transition is an order of magnitude or more greater than for those below transition and extends farther into the plasma (MHz peaks were not observed beyond 1 mm from the anode for conditions below transition). To further clarify the transition, Figure 4a plots the noise peaks at 0.1 mm shown in Figure 3 as a function of $\xi$ along with similar data obtained with a copper anode. It is interesting to note that the copper anode appears to transition at a lower $\xi$ value than the aluminum. This is also evident in Figure 4b in which data points are obtained by integrating noise spectra recorded at 0.1 mm over the range from 50 kHz to 2 MHz, followed by normalization with the dc current level (error bars are not presented for this highly qualitative data). The apparent early transition of copper will be demonstrated again in section 3.2.3 and discussed in section 3.2.7.

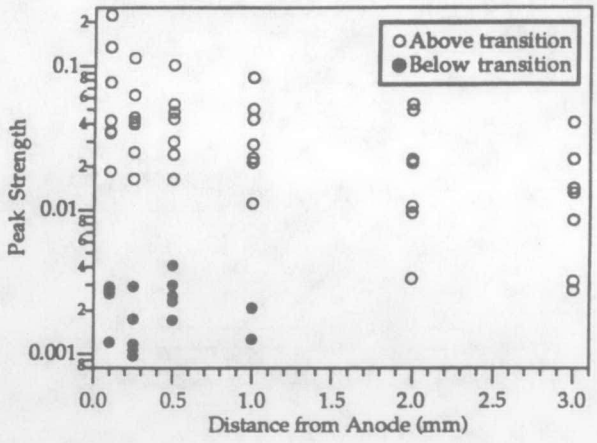


Figure 3: Amplitudes of consistently observed 2, 3, 4, and 7 MHz peaks for $\xi$ values both above and below transition near aluminum anode.

## 3.2 Spot Mode

### 3.2.1 Vacuum Arcs and Spot-Induced Noise

Anode mode transition is a widely observed and well documented phenomenon in vacuum arcs. An excellent review of vacuum arc anode phenomena, including discussion of a number of points of considerable relevance to our work, is provided by Miller [24]. Vacuum arcs (also known as metal vapor arcs) are discharges fed entirely by material burned off the electrodes, and find application primarily as high current circuit interrupters. At low currents spot attachments at the cathode supply the plasma which is collected in a diffuse mode by a passive anode. As the current is increased spots form at the anode, resulting in evaporation of anode material. The transition to the spot mode is marked by a sudden increase in the arc terminal voltage and in terminal voltage fluctuations [25]. Harris has demonstrated a direct

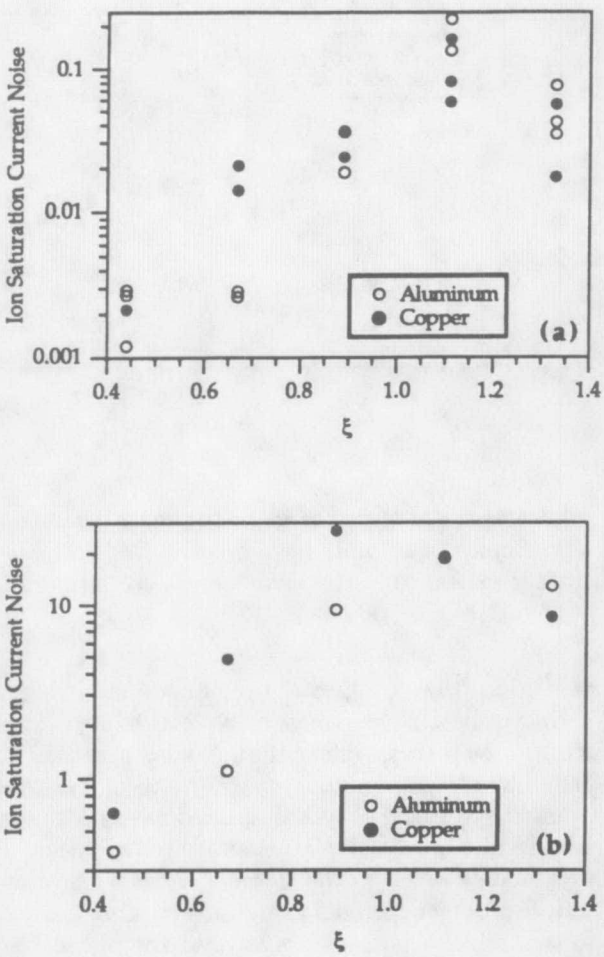


Figure 4: Ion saturation current noise at 0.1 mm from aluminum and copper anodes: a) peak amplitudes and b) integrated over 50 kHz to 2 MHz.

link between terminal noise and the appearance of transient luminous spots on the anode of a vacuum arc with copper electrodes [26]. Harris also shows that the frequency of oscillations in luminosity corresponds directly to the frequency of terminal voltage fluctuations, and that this frequency is near 100 kHz and is insensitive to variations in arc current. Harris mentions that significant components at higher frequencies are present, but does not identify their nature.

We consider the noise observed near our thruster anode to be the result of spot extinction and reignition (spot motion). Comparison of ion saturation current fluctuation spectra recorded with argon and helium propellants at the same values of $\xi$ show no appreciable differences in MHz level frequency content (Figure 5), indicating that it is unlikely that the noise originates from a natural plasma oscillation, since oscillations at frequencies of a few MHz in our plasma would very likely be dependent upon ion mass. A distinction does arise at frequencies below 1 MHz where sharp peaks are prominent only in the helium spectra. Similar results were obtained in Ref [22] in which voltage fluctuation spectra recorded with argon and hydrogen are shown to be nearly identical in the MHz range, while sharp peaks at a few hundred kHz are very prominent only in the hydrogen data. Another interesting feature of the work done in Ref [22] and of our work is that spectral content in the MHz range is found to be nearly independent of thruster current and mass flow. We do not even observe appreciable variation in spectral content (frequencies less than 10 MHz) between copper, aluminum, and molybdenum anodes. An investigation of the dependencies of spot jumping frequencies may clarify these observations.

### 3.2.2 Physical Evidence for Spot Mode

To test the spot hypothesis, a simple experiment was devised in which highly polished anodes were observed before and after 10 thruster firings at the same conditions used in the noise experiment ($\xi$ from 0.44 to 1.33 at 6 g/s mass flow). Spot damage visible to the unaided eye (spots on the order of 1 mm in diameter) was evident for $\xi$ values of 0.89, 1.11, and 1.33, but not for $\xi = 0.44$ and 0.67 with aluminum and copper anodes [27]. Spot damage was found almost exclusively on the anode lip. Spectroscopic erosion studies performed on the same thruster used in our work confirm that emission lines corresponding to anode material (aluminum) appear at a current of 16 kA when the thruster is fed 6 g/s argon ($\xi = 0.89$) with a propellant mass distribution similar to ours [28].

### 3.2.3 Trigger for Transition

The spot hypothesis appeared to merit further investigation, particularly with regard to the identification of a trigger for the transition. Vacuum arc researchers generally concern themselves with the effects of electrode material and geometry on the transition current and do not often employ plasma diagnostics in the inter-electrode gap. As a result there is not much information regarding a universal scaling parameter for the transition. However, it has been postulated that the ratio of the discharge current density $j$ to the thermal electron current density $j_{th}$ governs the

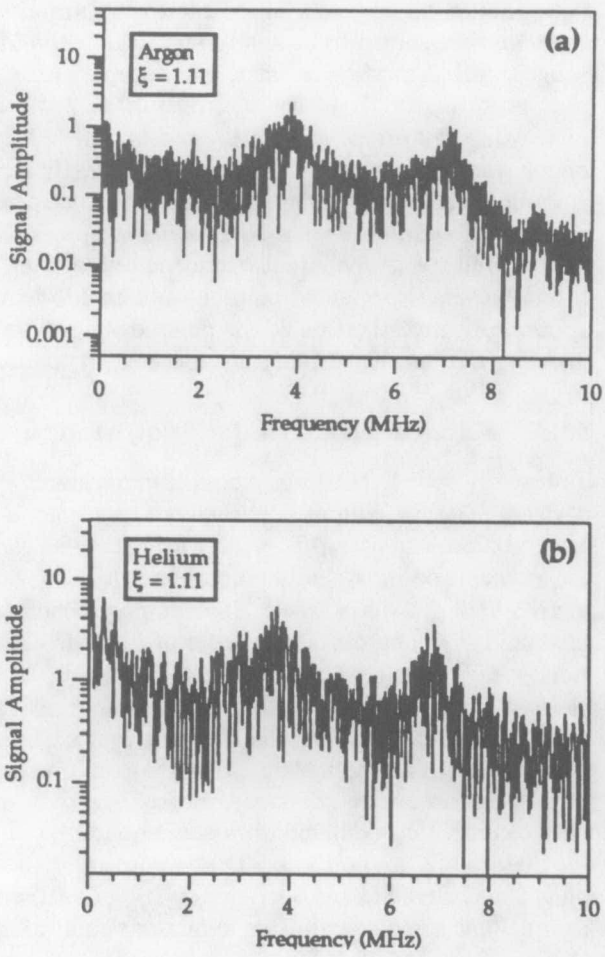


Figure 5: Ion saturation current noise at 0.1 mm from aluminum anode for $\xi = 1.11$: a) Argon and b) Helium. Spectra not normalized by dc saturation current.

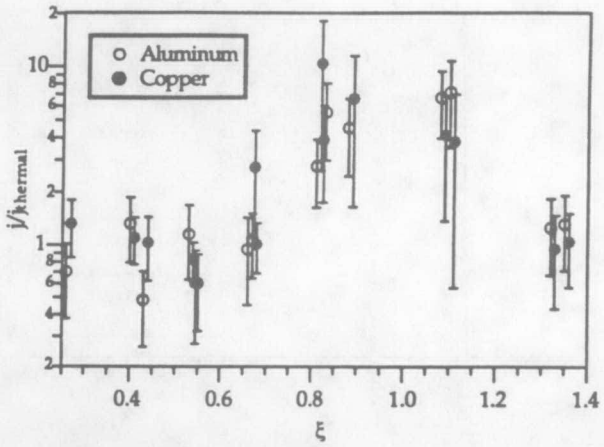


Figure 6: Ratio of discharge to thermal current density. Some data points have been shifted in $\xi$ value by 0.01 or less to clarify error bar placement.

transition [10, 12, 29]. Since the anode fall is largely a Debye-sheath phenomenon, we can look to Langmuir probe theory, which tells us that the current collected by a planar conductor (the ratio of the anode lip radius to Debye length is approximately 5000) immersed in a quiescent plasma saturates at a level approximately equal to the thermal current. Attempts to collect larger currents result in very large increases in the collector potential relative to the plasma, and corresponding increases in the energy input to the collector surface. At some point the input energy becomes sufficient to cause local overheating and significant evaporation of collector material. Following ionization by incoming electrons (due to uncertainty in the spot plasma density, it is unclear whether in our work the anode sheath voltage contributes to ionization of evaporated anode material, or if ionization is accomplished thermally outside the sheath), this material contributes to an increase in current to the evaporative region, leading to enhanced evaporation. This "runaway" effect results in spot formation [30].

Measurements of the discharge current density have been made at a distance of 1 mm from aluminum and copper anodes and are compared in Figure 6 to the thermally available electron currents calculated from plasma densities and temperatures measured 0.1 mm from the anode. This comparison has been done by other researchers with the result that the thermal current density equaled or exceeded the discharge current density [7, 9]. The reason for this is

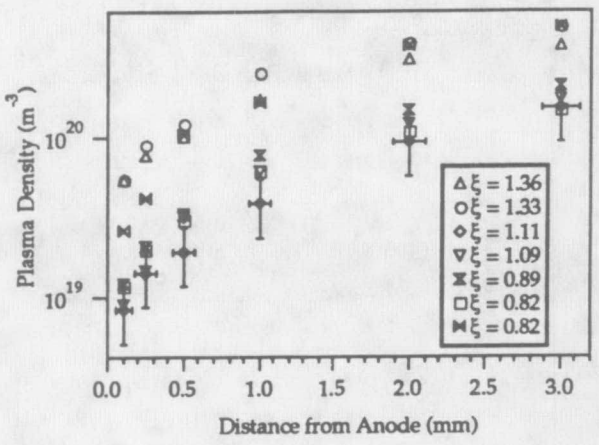


Figure 7: Plasma densities near aluminum anode (error bars represent average error for all conditions shown).

that their values of the thermal current density were based on values of plasma density recorded at least 1 mm from the anode surface. We have found that for all the conditions we have studied, substantial gradients in the plasma density exist within 1 mm of the anode. Figure 7 shows this for a few conditions with an aluminum anode (error bars on $\xi = 1.11$ data represent average error for all conditions shown). We believe that these gradients are established by the axial current crossed with azimuthal magnetic field ($j_z \times B_\theta$) pumping force (estimates of the magnitude of $j_z \times B_\theta$ near the anode compare favorably with measured pressure gradients), so that values of $j_{th}$ based on plasma properties recorded too close to the anode surface to be influenced by magnetic effects should provide the best estimates of conditions at the sheath edge. Figure 6 shows that indeed for the conditions below transition the ratio $j/j_{th}$ is close to 1, while at the point of transition values from 3 to 10 are achieved. With increases in $\xi$, the ratio actually returns to 1 (due to the density resurgence). This apparent contradiction will be discussed in section 3.2.4.

Another interesting point to note about Figure 6 concerns the data point corresponding to the copper anode operating at $\xi = 0.67$, which indicates that the copper anode should have transitioned at that operating condition. During the polished anode experiment, the copper anode did not show visible damage after 10 firings at $\xi = 0.67$. However, as previously mentioned there is evidence for transition in the noise data, and careful inspection of Figure 2a reveals that the anode fall for $\xi = 0.67$ lies midway between other values recorded before and after transition. It is possible that copper at $\xi = 0.67$ is in the early stages of transition, although it is puzzling that data at $\xi = 0.68$ returns to $j/j_{th}$ near one. Further evidence for the material dependence of transition will be presented in conjunction with the discussion of the behavior of the molybdenum anode (section 3.2.7).

It is not immediately obvious that the anode should be subject to current saturation. After all, the electrons are actually streaming toward the anode with velocities comparable to the electron thermal velocity (the ratio $j/j_{th}$ can be re-cast as the ratio of the electron drift velocity to the electron thermal velocity), and we might expect that the current collected by the anode would be given to a large extent by the product of the drift velocity with the plasma density, electron charge, and anode area. It is not entirely clear why the current collection should be diffusive, resulting in the buildup of charge (and potential) due to reliance on this insufficiently effective means of draining the charge into the anode. We postulate that the large Hall parameters present near the anode surface direct the electron drift velocity axially along the anode, forcing conduction into the lip to be via diffusion.

### 3.2.4 Resurgence of Plasma Density and $j_{th}$

As mentioned previously, $j/j_{th}$ returns to values near one at $\xi > 1.3$, presenting us with an apparent contradiction. We can provide the following explanation in terms of how the spot mode develops and the manner in which plasma properties were measured. Figure 8a is an unfiltered time history of the ion saturation current collected during a thruster firing at a condition below transition. The trace is quiescent in comparison to the same measurement, shown in Figure 8b, taken at a condition just above transition. These data were recorded during the period between approximately 700 and 900 microseconds into a one millisecond pulse. The trace in Figure 8b is punctuated, roughly at a frequency of 100 kHz, by excursions up to an order of magnitude larger than the dc level. We attribute these excursions to the passage of spots by the probe location. Further increases in $\xi$ result in traces dominated by the excursions, due either to enhanced spot motion or an increase in the number of spots (studies of cathode spots in vacuum arcs indicate that the current carried by an individual spot may have a limiting value, resulting in an

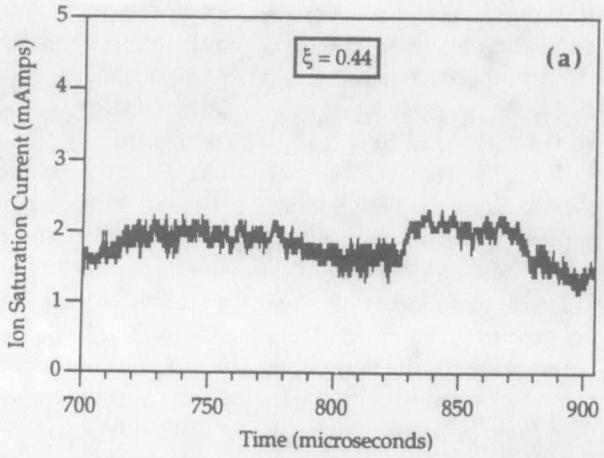


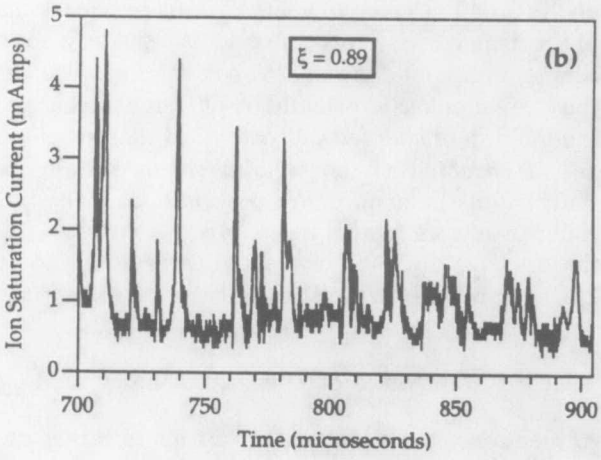


Figure 8: Ion saturation current time histories for: a) $\xi = 0.44$ and b) $\xi = 0.89$ with aluminum anode.

increase in the number of spots in response to increasing demands of the discharge [31]). The probe used to measure the ion saturation current is equipped with a filter that heavily attenuates signals in the range of 100 kHz. As a result, the intermittent excursions of Figure 8b are essentially invisible to the electronics and the recorded values will reflect the low-density plasma outside of the spots. With increasing $\xi$ the more intense spot vapor production results in probe readings which, after the usual filtering and averaging, display the net effect of the spot action, which is to solve the starvation crisis.

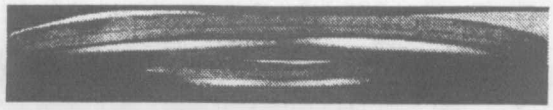

Figure 9: Roughened copper anode before firing.

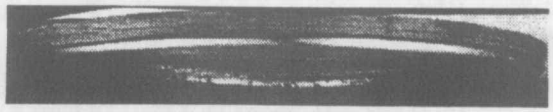

Figure 10: Roughened copper anode showing spot damage after 10 firings at $\xi = 0.44$.

### 3.2.5 Experiments with a Roughened Anode

To further investigate the spot mode, we roughened the anode surface in an attempt to produce a condition which would favor transition by providing preferential points of attachment. A knurling tool was run over the anode surface, producing roughness on a scale of approximately 0.1 mm. Inspection of freshly polished then roughened aluminum and copper anodes before and after 10 thruster firings at all of the conditions studied ($\xi$ values of 0.44, 0.67, 0.89, 1.33, and 1.36 with 6 g/s argon mass flow) indicated the presence of the spot mode. Figures 9 and 10 are before and after photos of a roughened copper anode operating at $\xi = 0.44$, a condition at which smooth anodes did not transition. Figure 10 shows clear evidence of spot damage on the anode lip.

Inducing the spot mode impacted both the thruster noise level and terminal voltage. Figure 11 is a comparison of integrated noise (over the range from 50 kHz to 2 MHz) for the smooth and roughened anodes. For conditions in which the smooth anodes did not transition, the roughened anodes exhibit significantly more noise, by an order of magnitude at $\xi = 0.44$. This is further evidence that the noise accompanying transition is directly associated with the spots. Figure 12a shows thruster terminal voltages for smooth and roughened aluminum anodes as a function of $\xi$. At low values of $\xi$ the roughened anode terminal voltage exceeds that of the smooth anode by a few volts, perhaps due to increased plasma resistivity produced by excessive evaporation of anode material. At the two highest values of $\xi$, however, the terminal voltage is substantially decreased. Experiments with the copper anode show very similar behavior. Comparison of plasma potentials recorded a few millimeters

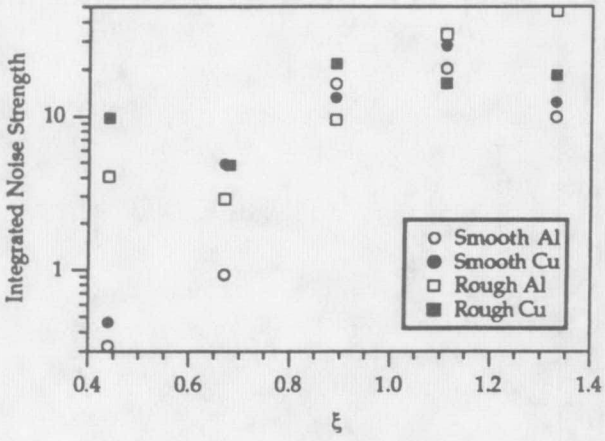


Figure 11: Ion saturation current noise 0.25 mm from rough and smooth aluminum and copper anodes.

from smooth and roughened aluminum anodes (Figure 12b) confirm that these changes are occurring in the anode region.

### 3.2.6 Anode Fall and Anode Vaporization

If we assume that the anode fall in the spot mode is established by the minimum input energy required to heat the anode surface to the point where significant evaporation of anode material occurs, then an explanation for the reduced anode falls obtained with roughened anodes appears quite readily. For a given input power, metal whiskers produced by the roughing will reach higher temperatures at their extremities because of the low cross-sectional area of heat conduction paths into the body of the anode (power input to the whiskers is undoubtedly also enhanced by local electric field concentrations). Lower anode falls are thus required to achieve temperatures required for significant vaporization. This of course also explains the early transition of the roughened anodes, which allow vaporization even at the low input power available from a sheath that has not yet reached current saturation. Smooth anodes, on the other hand, appear to require the increased power available from the large increases in sheath voltage that accompany current saturation.

It is very interesting to try to quantify what temperatures should be required for "significant" vaporization. If we assume that the temperature should be such that the equilibrium vapor density is comparable to measured values of the plasma density

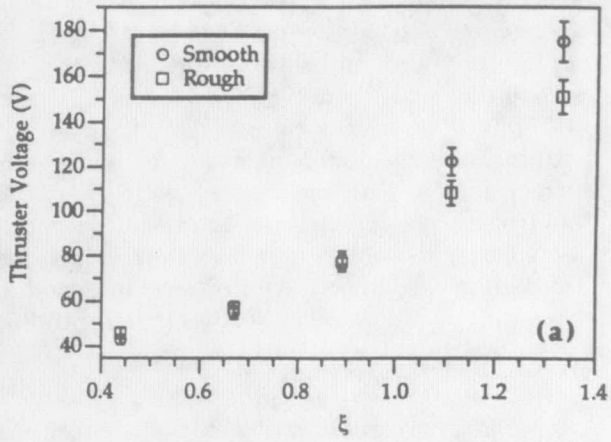


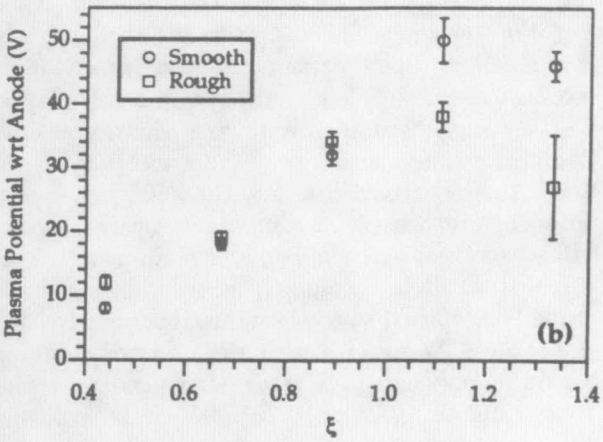


Figure 12: Smooth and roughened aluminum anodes: a) thruster terminal voltage and b) plasma potential a few millimeters from anode surface.

near the anode [29], then for both the copper and aluminum anodes we obtain values close to 1400 K (evaporation is such a strong function of temperature that order of magnitude changes in vapor density require less than a 10 percent adjustment to this value [32, 33]). Two points can be made with regard to this value. The first is that the melting points of aluminum and copper are 934 K and 1357 K respectively. This is in accord with experimental observations of gross melting associated with spot attachments on the aluminum anode, where material has clearly been splashed about. Gross melting, however, was never observed on the copper anode. Only darkened abrasions were visible at the points of spot attachment. The second point is that if we

very simplistically model the anode as a semi-infinite solid with a constant applied heat flux (determined by the product of current density with the anode fall, electron enthalpy, and surface work function), then we find that in order to obtain surface temperatures near 1400 K in the course of a 1 millisecond firing with measured values of the anode fall and electron temperature we must require constriction of the current density by approximately an order of magnitude above values measured 1 mm from the anode surface. This is of course in accord with the spot hypothesis and with the size of the excursions in ion saturation current shown in Figure 8b.

### 3.2.7 Experiments with a Molybdenum Anode

**Anode Fall** Data regarding the material dependence of the anode fall lead naturally to the conclusion that low vapor pressure anode materials should exhibit larger anode falls in the spot mode. A molybdenum anode was chosen to test this hypothesis. Equilibrium vapor pressure data for molybdenum indicate that a temperature near 2800 K is required to produce vapor densities comparable to plasma densities measured near copper and aluminum anodes. Application of the simple heat transfer model described previously, with an assumed spot current density of 2000 A/cm$^2$ (approximately an order of magnitude larger than measured values) indicates that anode falls in excess of 80 volts might be expected. Values this large were not observed, however it is clear from Figure 13 that for conditions above transition, anode falls measured with the molybdenum anode exceed those with copper and aluminum anodes by a substantial margin. Accurate determination of spot current densities (which would provide more reliable estimates of required anode falls) is a difficult task which has received considerable attention with regard to cathode spots, for which published values can vary by several orders of magnitude [34].

**Early Transition** The molybdenum anode also transitions earlier than the copper and aluminum anodes. As previously mentioned, noise and anode fall data with the copper anode at $\xi = 0.67$ seemed to indicate transition in progress, however no damage visible to the unaided eye was observed on the anode surface. In contrast, physical damage was observed on the molybdenum anode after operation at $\xi = 0.67$. Much like the copper anode, this damage did not involve gross anode melting, in accordance

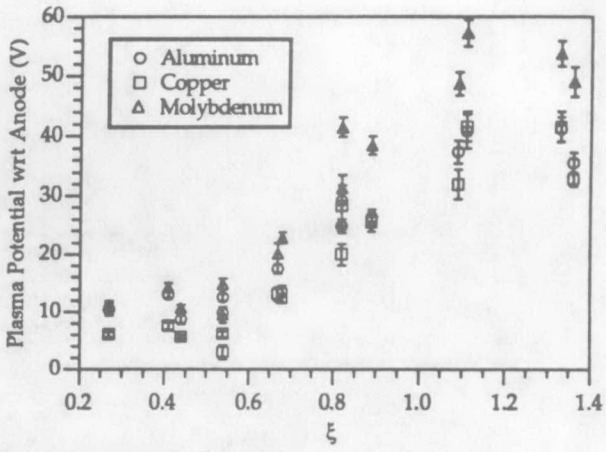


Figure 13: Plasma potentials 0.5 mm from aluminum, copper, and molybdenum anodes.

with the estimated surface temperature requirement (2800 K) lying below the melting point of molybdenum (2896 K). The transition is marked by the appearance of anode falls in excess of 20 volts (Figure 13) and an order of magnitude increase in anode noise compared to operation at $\xi = 0.44$ (Figure 14).

The early transition of molybdenum is another apparent contradiction when viewed in terms of the results of experiments aimed at determining the dependence of the threshold current for anode spot formation in vacuum arcs on anode thermal properties. The spotting observed on our anode is more reminiscent of the footpoint mode described by Miller [24] than it is of the gross spot formation dealt with in these transition studies, however the results, which are that the critical current for the appearance of a gross spot increases with the thermal characteristic $T_m(k\rho c)^{1/2}$ [35], are relevant since the footpoint mode is considered to be a precursor to gross spotting. $T_m$, $k$, $\rho$, and $c$ represent the melting point, thermal conductivity, density, and specific heat of the anode respectively, and $T_m(k\rho c)^{1/2}$ for molybdenum exceeds that of aluminum by more than a factor of three, indicating that molybdenum should transition at a higher current than aluminum. This apparent contradiction can be explained by consideration of how the vacuum arc data is obtained. Typically a half-sinusoidal current pulse of limited duration is supplied to the arc. Spot formation requires a certain energy input to heat the anode. Since the energy input is over a fixed time interval, anode materials requiring greater input en-

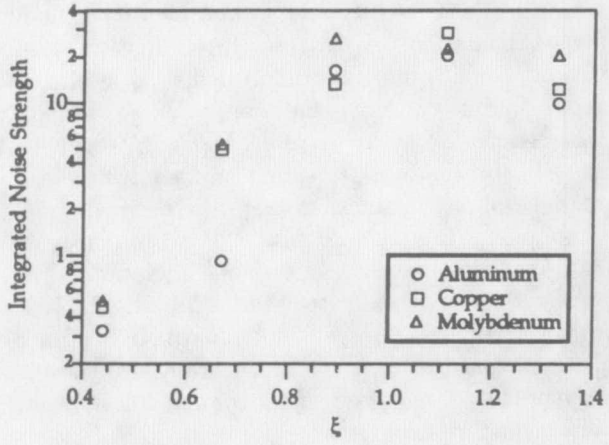


Figure 14: Integrated ion saturation current noise (50 kHz to 2 MHz) 0.25 mm from aluminum, copper, and molybdenum anodes.

ergy will require correspondingly higher power, with the result that the more refractory metals appear to have higher transition currents. This result is relevant to arc engineering, but not to the mechanism controlling transition (which we consider to be current saturation for smooth anodes), and thus does not prohibit our observations. We postulate that the material dependence of the point of transition arises from anode erosion in the diffuse mode. The relatively higher vapor pressure of aluminum at low temperature may supply the discharge with sufficient material to postpone the criticality of $j/j_{th}$ to higher $\xi$ values than for copper or molybdenum (data permitting calculation of $j/j_{th}$ for molybdenum have not been taken).

**Noise** Another prediction that we have investigated regarding spot behavior is that low vapor pressure materials may be noisier than higher vapor pressure materials [35]. As previously mentioned, we consider spot extinction and reignition to be responsible for noise production. Theories regarding the motion of cathode spots generally invoke interactions between the spot current and magnetic fields induced by the global discharge current and/or by the local spot current [36, 37]. It is possible that as a spot becomes a more prolific generator of anode vapor, the resultant increase in collisionality will cause magnetic effects to diminish in importance and the spot may root itself more firmly to the anode. Spots on a high vapor pressure material may exhibit less mobility and consequently lower noise generation than those on a low vapor pressure material. This prediction is not borne out by the data of Figure 14, however this data only covers the frequency range from 50 kHz to 2 MHz. In an attempt to investigate the widest possible spectrum of noise, ion saturation current data were fed in real time to an analog spectrum analyzer covering the range from 0 to 50 MHz. Photographs of the analyzer output with aluminum and molybdenum anodes operating at $\xi = 1.11$ are shown in Figure 15. The ordinate in these photographs is a logarithmic scale. While many characteristics of the spectra are similar, it is apparent that the molybdenum anode is noisier, particularly in the range from 15 to 20 MHz. This is typical of spectra recorded at $\xi$ values of 0.89 and 1.33 as well.

### 3.2.8 Anode Fall Saturation

A final observation may be made with regard to another very widely observed and well documented behavior in vacuum arcs, namely that with increasing current after transition, the arc noise level and arc terminal voltage both decrease substantially, presumably due to intense spot attachment with prolific vapor generation [25]. This behavior is observed in the data of Figures 2a, 4a, 4b, 11, 13, and 14, which show that the anode fall and near-anode noise level reach a peak and then decrease at the highest $\xi$ values studied. Other researchers have observed anode fall saturation [9, 14] and Gallimore [9] has associated it with the decrease of the anode power fraction with increasing thruster power. We believe that the spot mode provides a very plausible mechanism for anode fall saturation.

## 4 Conclusion

Plasma properties near the smooth aluminum and copper anodes of a high power pulsed MPD thruster indicate that the anode transitions from a mode of diffuse, low voltage, and low noise current collection to one of high voltage, high noise, and spotty current attachment. The mode transition is triggered by anode sheath current saturation, which results in increasing power to the anode surface until local heating and vaporization generate spots, resulting in a limitation of the anode sheath voltage to values required to vaporize sufficient anode material to solve the starvation crisis. Starvation is precipitated by another runaway phenomenon, $j_z \times B_\theta$ pumping (i. e.

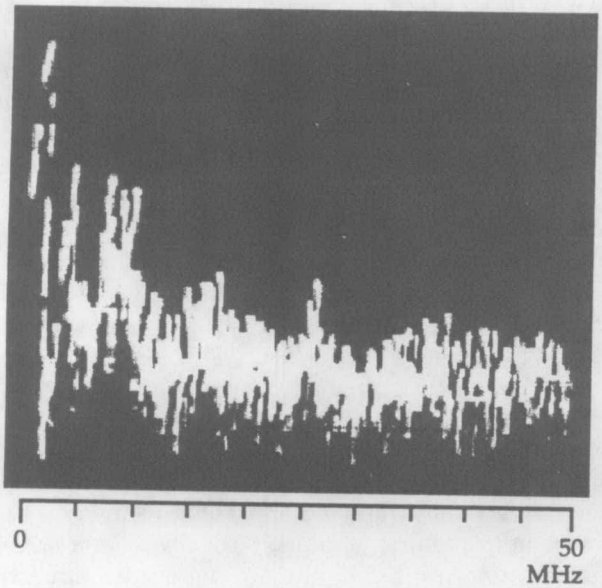


Figure 15: Ion saturation current noise spectra, $\xi = 1.11$ (ordinate is a logarithmic scale). Top photo: aluminum, Bottom photo: molybdenum.

reductions in density lead to increasing Hall parameters which lead to increasing $j_z$ and $B_\theta$ which further decreases plasma density, etc. ). Premature induction of the spot mode accomplished by roughing the anode surface confirms that the increased discharge noise associated with this mode is generated by spot motion, and that anode vaporization controls the anode fall voltage in the spot mode. Experiments with a molybdenum anode confirm the expectation that anode falls in the spot mode should increase and become noisier as the anode material becomes more refractory. Finally, the spot mode is found to provide a mechanism for anode fall saturation and the consequent decrease of the anode power fraction with increasing thruster power.

**Acknowledgments** The authors would like to thank George E. Miller for his invaluable assistance in the laboratory. This work has been supported in part by the Fannie and John Hertz Foundation.

## References

[1] J.H. Gilland. Mission and system optimization of nuclear electric propulsion vehicles for lunar and mars missions. In *22nd International Electric Propulsion Conference*, Viareggio, Italy, October 14-17 1991. IEPC-91-038.

[2] J. Sercel and S. Krauthamer. Multimegawatt nuclear electric propulsion; first order system design and performance evaluation. In *AIAA Space Systems Technology Conference*, San Diego, California, June 9-12 1986. AIAA-86-1202.

[3] D.Q. King and J.C. Sercel. A review of the multimegawatt MPD thruster and current mission applications. In *22nd Joint Propulsion Conference*, Huntsville, Alabama, June 16-18 1986. AIAA-86-1437.

[4] L.K. Rudolph and K.M. Hamlyn. A comparison between advanced chemical and MPD propulsion for geocentric missions. In *19th Joint Propulsion Conference*, Seattle, Washington, June 27-29 1983. AIAA-83-1391.

[5] E.Y. Choueiri, A.J. Kelly, and R.G. Jahn. Mass savings domain of plasma propulsion for LEO to GEO transfer. *Journal of Spacecraft and Rockets*, 30(6):749–754, Nov.-Dec. 1993.

[6] J.S. Sovey and M.A. Mantenieks. Performance and lifetime assessment of magnetoplasmadynamic arc thruster technology. *J. Propulsion*, 7(1):71–83, Jan.-Feb. 1991.

[7] R.C. Oberth. *Anode Phenomena in High-Current Discharges.* PhD thesis, Princeton University, December 1970.

[8] A.J. Saber. *Anode Power in a Quasi-Steady MPD Thruster.* PhD thesis, Princeton University, May 1974.

[9] A.D. Gallimore. *Anode Power Deposition in Coaxial MPD Thrusters.* PhD thesis, Princeton University, October 1992.

[10] H. Hugel. Effect of self-magnetic forces on the anode mechanism of a high current discharge. *IEEE Transactions on Plasma Science*, PS-8(4):437–442, December 1980.

[11] F.G. Baksht, B. Ya. Moizhes, and A.B. Rybakov. Critical regime of a plasma accelerator. *Soviet Physics Technical Physics*, 18(12):1613–1616, June 1974.

[12] L.I. Vainberg, G.A. Lyubimov, and G.G. Smolin. High-current discharge effects and anode damage in an end-fire plasma accelerator. *Soviet Physics Technical Physics*, 23(4):439–443, April 1978.

[13] E.Y. Choueiri, A.J. Kelly, and R.G. Jahn. The manifestation of Alfven's hypothesis of critical ionization velocity in the performance of MPD thrusters. In *18th International Electric Propulsion Conference*, Alexandria, Virginia, Sept. 30 - Oct. 2 1985. AIAA-85-2037.

[14] K. Kuriki and M. Onishi. Thrust measurement of K III MPD arcjet. In *15th International Electric Propulsion Conference*, Las Vegas, Nevada, April 21-23 1981. AIAA-81-0683.

[15] A.C. Malliaris, R.R. John, R.L. Garrison, and D.R. Libby. Performance of quasi-steady MPD thrusters at high powers. *AIAA Journal*, 10(2):121–122, February 1972.

[16] E.Y. Choueiri, A.J. Kelly, and R.G. Jahn. MPD thruster plasma instability studies. In *19th International Electric Propulsion Conference*, Colorado Springs, Colorado, May 11-13 1987. AIAA-87-1067.

[17] J.W. Barnett and R.G. Jahn. Onset phenomena in MPD thrusters. In *18th International Electric Propulsion Conference*, Alexandria, Virginia, Sept. 30 - Oct. 2 1985. AIAA-85-2038.

[18] M. Wolff, A.J. Kelly, and R.G. Jahn. A high performance magnetoplasmadynamic thruster. In *17th International Electric Propulsion Conference*, Tokyo, Japan, 1984. IEPC-84-32.

[19] D.Q. King, W.W. Smith, R.G. Jahn, and K.E. Clark. Effect of thrust chamber configuration on MPD arcjet performance. In *14th International Electric Propulsion Conference*, Princeton, New Jersey, Oct. 30 - Nov. 1 1979. AIAA-79-2051.

[20] K.D. Diamant, E.Y. Choueiri, A.J. Kelly, and R.G. Jahn. Characterization of the near-anode region of a coaxial MPD thruster. In *30th Joint Propulsion Conference*, Indianapolis, Indiana, June 27-29 1994. AIAA-94-3336.

[21] E.C. Bowman and D.L. Tilley. Microinstabilities in high power MPD systems: Preliminary diagnostics. In *23rd International Electric Propulsion Conference*, Seattle, Washington, September 1993. IEPC-93-125.

[22] K. Kuriki and H. Iida. Spectrum analysis of instabilities in MPD arcjet. In *17th International Electric Propulsion Conference*, Tokyo, Japan, 1984. IEPC-84-28.

[23] H.L. Kurtz, M. Auweter-Kurtz, W.D. Merke, and H.O. Schrade. Experimental MPD thruster investigations. In *19th International Electric Propulsion Conference*, Colorado Springs, Colorado, May 11-13 1987. AIAA-87-1019.

[24] H.C. Miller. A review of anode phenomena in vacuum arcs. *IEEE Transactions on Plasma Science*, PS-13(5):242–252, October 1985.

[25] G.R. Mitchell. High-current vacuum arcs: Part I—an experimental study. *Proc. IEE*, 117(12):2315–2326, December 1970.

[26] L.P. Harris. Small-scale anode activity in vacuum arcs. *IEEE Transactions on Plasma Science*, PS-10(3):173–180, September 1982.

[27] K.D. Diamant. Report No. EPPDyL-TR-95S. Technical report, Mechanical and Aerospace Engineering Dept., Princeton University, January-June 1995. To be Published.

[28] D.D. Ho. Erosion studies in an MPD thruster. Master's thesis, Princeton University, May 1981.

[29] G.A. Dyuzhev, G.A. Lyubimov, and S.M. Shkol'nik. Conditions of the anode spot formation in a vacuum arc. *IEEE Transactions on Plasma Science*, PS-11(1):36–45, March 1983.

[30] J.M. Lafferty. Triggered vacuum gaps. *Proceedings of the IEEE*, 54(1):23–32, January 1966.

[31] J.M. Lafferty, editor. *Vacuum Arcs: Theory and Application.* John Wiley and Sons, 1980. pp. 120-121.

[32] W.M. Rohsenow, J.P. Hartnett, and E.N. Ganic, editors. *Handbook of Heat Transfer Fundamentals.* McGraw-Hill, 2nd edition, 1985. page 3-124.

[33] S. Dushman and J.M. Lafferty, editors. *Scientific Foundations of Vacuum Technique.* John Wiley and Sons, 1962. Chap. 10.

[34] E. Hantzsche and B. Juttner. Current density in arc spots. *IEEE Transactions on Plasma Science*, PS-13(5):230–234, October 1985.

[35] J.A. Rich, L.E. Prescott, and J.D. Cobine. Anode phenomena in metal-vapor arcs at high currents. *Journal of Applied Physics*, 42(2):587–601, February 1971.

[36] H.O. Schrade, M. Auweter-Kurtz, and H.L. Kurtz. Cathode phenomena in plasma thrusters. In *19th International Electric Propulsion Conference*, Colorado Springs, Colorado, May 11-13 1987. AIAA-87-1096.

[37] L.P. Harris. Transverse forces and motions at cathode spots in vacuum arcs. *IEEE Transactions on Plasma Science*, PS-11(3):94–102, September 1983.